EXTENDED PDF FORMAT
SPONSORED BY
usb
Products from Affymetrix
www.usbweb.com

A Role for the ESCRT System in Cell Division in Archaea

Rachel Y. Samson, *et al.*

Science **322**, 1710 (2008);
DOI: 10.1126/science.1165322

The following resources related to this article are available online at www.sciencemag.org (this information is current as of December 18, 2008):

Updated information and services, including high-resolution figures, can be found in the online version of this article at:
http://www.sciencemag.org/cgi/content/full/322/5908/1710

Supporting Online Material can be found at:
http://www.sciencemag.org/cgi/content/full/1165322/DC1

This article **cites 21 articles**, 4 of which can be accessed for free:
http://www.sciencemag.org/cgi/content/full/322/5908/1710#otherarticles

This article appears in the following **subject collections**:
Cell Biology
http://www.sciencemag.org/cgi/collection/cell_biol

Information about obtaining **reprints** of this article or about obtaining **permission to reproduce this article** in whole or in part can be found at:
http://www.sciencemag.org/about/permissions.dtl

Downloaded from www.sciencemag.org on December 18, 2008

Science (print ISSN 0036-8075; online ISSN 1095-9203) is published weekly, except the last week in December, by the American Association for the Advancement of Science, 1200 New York Avenue NW, Washington, DC 20005. Copyright 2008 by the American Association for the Advancement of Science; all rights reserved. The title *Science* is a registered trademark of AAAS.

16. Microchannels enable cell confinement during motion and therefore mimic the microenvironment encountered by DCs in the constrained interstitial spaces of peripheral tissues and lymphoid organs. They impose a directional migration to cells, which facilitates the extraction of measurable parameters. DCs entered and moved spontaneously and bidirectionally along microchannels, with their cell body being constrained during motion (fig. S4). Time-lapse movies obtained with WT, $Ii^{-/-}$, and $CatS^{-/-}$ DCs were analyzed by drawing kymographs and extracting cell positioning and instantaneous velocity data for individual migrating cells with a specialized computer program (figs. S4 and S5).
17. M. Boes *et al*., *Eur. J. Immunol.* **35**, 2552 (2005).
18. K. Clark, M. Langeslag, C. G. Figdor, F. N. van Leeuwen, *Trends Cell Biol.* **17**, 178 (2007).
19. J. A. Villadangos *et al*., *Immunity* **14**, 739 (2001).
20. J. Jacobelli, S. A. Chmura, D. B. Buxton, M. M. Davis, M. F. Krummel, *Nat. Immunol.* **5**, 531 (2004).
21. M. M. Andzelm, X. Chen, K. Krzewski, J. S. Orange, J. L. Strominger, *J. Exp. Med.* **204**, 2285 (2007).
22. K. Krzewski, X. Chen, J. S. Orange, J. L. Strominger, *J. Cell Biol.* **173**, 121 (2006).
23. The authors thank T. Makushok for setting up the cell migration microchannel system; A. Azicune for cell micropatterning techniques; W. Faigle and D. Lowe for proteomics analysis; C. Recchi for help with gelatin-FITC degradation experiments; H. Overkleeft for synthesizing the LHVS; J. Roger for providing magnetic nanoparticles; M. Leberre, D. Baigl, and Y. Chen for help with microfabrication; and S. Amigorena, M. Sixt, P. Benaroch, V. Soumelis, C. Hivroz, and I. Fernandez for advice on the manuscript. A.-M.L.-D. thanks Y. Bellaïche for help with manuscript redaction. G.F.-A. was supported by a fellowship from the Ministère Français de la Recherche and, together with M.H., from the Association pour la Recherche contre le Cancer (ARC). P.V. and M.-I.Y. benefited from ECOS–Comisíon Nacional de Investigacíon Científica y Technológica, Gobierno de Chile fellowship (CO3S01), Institut Curie and Inserm fellowships, respectively. V.S. was part of the Leonardo Da Vinci project (Unipharma-Graduates, Sapienza University of Rome). This work was funded in part by grants from the ARC, Fondecyt (Chile) to M.-R.B. (1060834) and M.R. (1060253); Agence Nationale pour la Recherche (ANR-06-PCVI-0010) and Human Frontiers Science Program (RGY53/2007) to M.P.

Supporting Online Material

www.sciencemag.org/cgi/content/full/322/5908/1705/DC1
Materials and Methods
Figs. S1 to S11
References
Movies S1 to S7

1 May 2008; accepted 27 October 2008
10.1126/science.1159894

A Role for the ESCRT System in Cell Division in Archaea

Rachel Y. Samson,[1]* Takayuki Obita,[2] Stefan M. Freund,[3] Roger L. Williams,[2] Stephen D. Bell[1]*†

Archaea are prokaryotic organisms that lack endomembrane structures. However, a number of hyperthermophilic members of the Kingdom *Crenarchaea*, including members of the *Sulfolobus* genus, encode homologs of the eukaryotic endosomal sorting system components Vps4 and ESCRT-III (endosomal sorting complex required for transport–III). We found that *Sulfolobus* ESCRT-III and Vps4 homologs underwent regulation of their expression during the cell cycle. The proteins interacted and we established the structural basis of this interaction. Furthermore, these proteins specifically localized to the mid-cell during cell division. Overexpression of a catalytically inactive mutant Vps4 in *Sulfolobus* resulted in the accumulation of enlarged cells, indicative of failed cell division. Thus, the archaeal ESCRT system plays a key role in cell division.

Within the archaeal domain of life, there are two principal Kingdoms, the *Crenarchaea* and the *Euryarchaea*. Studies of microbial diversity have revealed that crenarchaea are one of the most abundant forms of life on Earth (*1*, *2*); however, we know essentially nothing about how cell division occurs in these organisms. This is of particular interest because the sequenced genomes of hyperthermophilic crenarchaeotes lack genes for members of the FtsZ/tubulin and MreB/actin superfamilies of cell division proteins (*3*–*6*). The near-ubiquity of tubulins and actins underscores these proteins' pivotal roles in cell division processes in bacteria, euryarchaea, and eukarya. The absence of orthologs of these proteins in the crenarchaea has prompted us to attempt to identify the crenarchaeal cell division machinery, using species of the genus *Suflolobus* as a model system. In metazoa, the ESCRT (endosomal sorting complex required for transport) system, in addition to its roles in endosomal trafficking and viral egress (*7*–*10*), plays a role in membrane abscission during cytokinesis (*11*–*13*). Most hyperthermophilic crenarchaea encode homologs of ESCRT-III components and the adenosine triphosphatase (ATPase) Vps4 (*14*, *15*) that could potentially be involved in cell division (figs. S1 to S3). *Sulfolobus* encodes four ESCRT-III homologs and a single Vps4 homolog. No homologs of the ESCRT-0, -I, or -II systems are apparent. The Vps4 gene is located within an operon-like structure with an ESCRT-III homolog and a third protein predicted to contain a coiled-coil structure (fig. S1).

First, we profiled the cell-cycle expression of the *Sulfolobus* ESCRT machinery in synchronized cultures of *Sulfolobus acidocaldarius* (*16*, *17*) (Fig. 1, A and B). Transcripts of Saci1372 (Vps4) and ESCRT-III homologs Saci1373, -0451, and -1416 underwent a characteristic modulation, with lowest levels in S phase–enriched populations (at the 30-min time point) and levels peaking between three and four times higher in populations enriched in dividing cells (at 180 min). In agreement with this result, levels of Saci1373 (ESCRT-III) protein were highest in dividing cell populations (Fig. 1C, upper panel). In contrast, Vps4 protein remained nearly constant across the cell cycle (Fig. 1C, middle panel). Immunostaining with antibodies to Saci1373 (ESCRT-III) revealed a distinct subcellular localization of the protein. More specifically, in cells where the two nucleoids had separated, a band or belt of Saci1373 (ESCRT-III) was detected between the two nucleoids, correlating with the site of membrane ingression (Fig. 2, figs. S5 and S6, and movie S1). Similar results were observed for Vps4 localization, although in addition to the strong staining at mid-cell, we generally observed a weaker, diffuse background distributed throughout the cell body (Fig. 2). The highly specific localization of these proteins to the mid-cell in dividing cells suggested a role in cell division–related processes.

In eukaryotes, ESCRT-III family proteins are capable of both homo- and heteromultimeric interactions resulting in the generation of protein lattices. We tested the ability of the four *Sulfolobus* ESCRT-III homologs to interact with one another using yeast two-hybrid assays (Fig. 3A). A series of interactions between these proteins was detected, indicating that the archaeal ESCRT-III proteins have the capacity to form an extended lattice. In eukaryotes, Vps4 plays a pivotal role in disassembling the ESCRT-III lattice and has been shown to interact with ESCRT-III proteins via the MIT domain of Vps4 and the C-terminal tails of ESCRT-IIIs. We tested whether the Saci1373 (ESCRT-III) and Vps4 proteins interact directly. Full-length (residues 1 to 261) Saci1373 (ESCRT-III) and Saci1372 (Vps4) did indeed interact (Fig. 3, B and C). The minimal interaction sites comprised residues 183 to 193 of Saci1373 (ESCRT-III), a notably hydrophobic and proline-rich region (Fig. 3B), and the MIT domain of Saci1372 (Vps4) (Fig. 3C). To better understand the basis of this interaction, we determined the co-crystal structure of the MIT domain of Saci1372 (Vps4) with a peptide corresponding to residues 183 to 193 of Saci1373 (ESCRT-III). The MIT domain forms a three-helix bundle, and the peptide binds in an extended configuration to the groove formed between helices α1 and α3 (Fig. 3D). The residues interacting with the MIT domain constitute part of a 183-(R/K)XLLP(D/E)LPXPP-193 motif (*18*) present in most orthologs of Saci1373. Among the four Saci ESCRT-III–like subunits, only Saci1373

[1]Medical Research Council (MRC) Cancer Cell Unit, Hills Road, Cambridge CB2 0XZ, UK. [2]MRC Laboratory of Molecular Biology, Hills Road, Cambridge, CB2 0QH, UK. [3]MRC Centre for Protein Engineering, Hills Road, Cambridge CB2 0QH, UK.
*Present address: Sir William Dunn School of Pathology, South Parks Road, Oxford, OX1 3RE, UK.
†To whom correspondence should be addressed. E-mail: stephen.bell@path.ox.ac.uk

Downloaded from www.sciencemag.org on December 18, 2008

has this MIT-binding motif (fig. S2). Two other ESCRT-III–like subunits (Saci1416 and Saci0451) bound the Saci1372 (Vps4) MIT domain with lower affinity, whereas Saci1601 does not bind (fig. S7). Pro^{187} of this motif is a *cis*-Pro that forces a sharp kink in the bound peptide so that Leu^{186} and Pro^{187} have only limited contact with the MIT domain. The core residues in contact with the MIT domain (189-LP-190) are essential for maintaining interaction with the MIT domain in solution (figs. S2 and S8). This mode of interaction is distinct from the previously characterized structures of complexes of yeast and human Vps4 MIT domains with interacting peptides [MIMs (MIT-interacting motifs)] derived from ESCRT-III family members Vps2 and human CHMP1A and -2B (*14*, *19*). In those structures, the MIM formed an amphipathic alpha helix that binds between α2 and α3 of the MIT domain (Fig. 3E). However, the MIM in human CHMP6 (termed MIM2) binds in an extended configuration along the groove formed by helices 1 and 3 of the MIT domain (*20*). Although the CHMP6 MIM2 lacks the *cis*-Pro equivalent of Saci1373 Pro^{187} and the corresponding kink of the main chain, the residues interacting with the Vps4 MIT domain and the extended main-chain conformations for these residues are essentially the same as we observe for Saci1373 binding to the Saci1372 (Vps4) (Fig. 3F). Despite the 2- billion-year evolutionary gulf between *Sulfolobus* Saci1373 (ESCRT-III) and human CHMP6, the sequences of the MIT-interacting peptides of these two proteins are clearly conserved at the primary sequence level.

Thus, archaeal ESCRT components are cell-cycle–regulated, interact via an evolutionarily conserved interface, and show specific subcellular localization to the site of membrane ingression during archaeal cell division. To further test the in vivo role of the *Sulfolobus* ESCRT components, we generated an episomal vector to direct arabinose-inducible expression of a target gene in *S. solfataricus* (*21*) (figs. S9 to S11). We transformed *S. solfataricus* with either an empty vector or vector containing wild-type Vps4 or an ATPase-defective [Glu^{206}→Gln^{206} (E206Q), "Walker B"] mutant of Vps4 (Fig. 4, A to C).

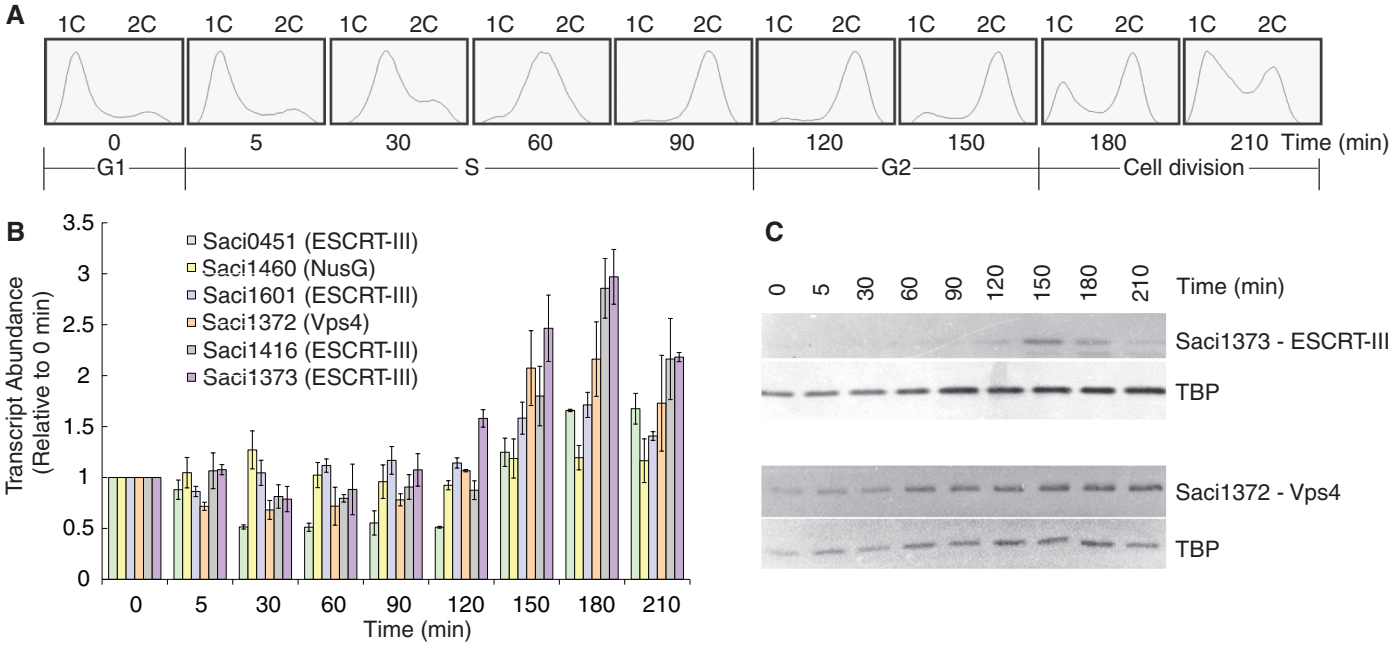

Fig. 1. (**A**) Flow cytometric analysis of samples taken at the indicated time points during the progression of a synchronized culture of *S. acidocaldarius*. The positions of peaks corresponding to one chromosome content (1C) and 2C genome contents are indicated. The cell-cycle stages are indicated at the bottom. (**B**) Real-time polymerase chain reaction measurements of transcript abundance of the indicated ESCRT-III homologs, Vps4, and a housekeeping control (the *nusG* transcription elongation factor). Experiments were performed in triplicate, and the SD is indicated by the error bars. All samples were normalized to the level detected at 0 min. (**C**) Western blot analysis of the levels of Saci1373 (ESCRT-III), Vps4, and the general transcription factor TATA box–binding protein (TBP) proteins across the cell cycle. Samples were taken at the indicated times during the growth of synchronized *S. acidocaldarius* cultures.

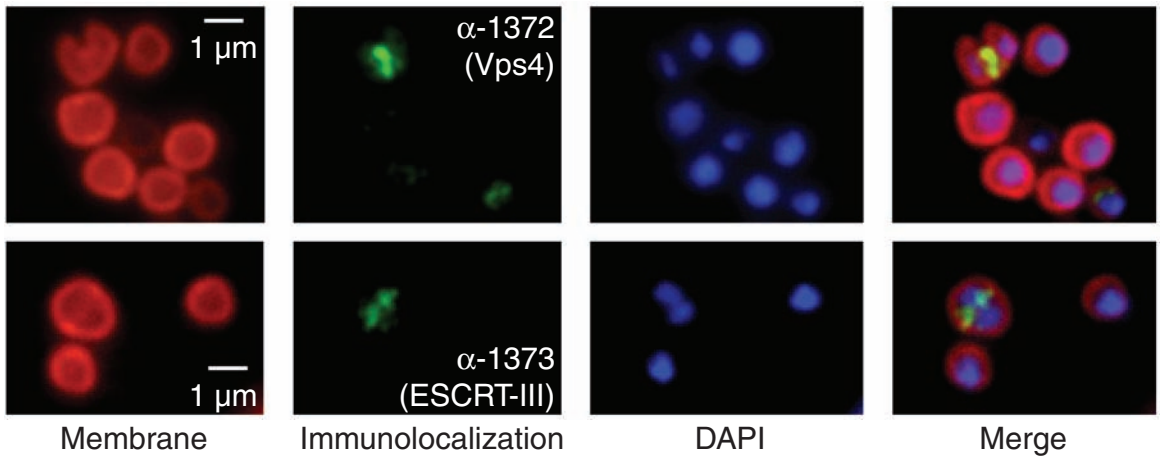

Fig. 2. Localization of (**Top**) Saci1372 (Vps4) and (**bottom**) Saci1373 (ESCRT-III). Representative images are shown. Images show the FM4-64X staining for membrane (red), DAPI staining for DNA (blue), antibody labeling of ESCRT-III or Vps4 (green), and merged images. Scale bar, 1 μm. Additional images are shown in figs. S6 and S7 and movie S1.

Downloaded from www.sciencemag.org on December 18, 2008

Overexpression of wild-type Vps4 results in the appearance of only a small proportion of enlarged cells with elevated DNA content, indicated by red triangles in Fig. 4B. Induction of the mutant Vps4 E206Q results in a far more dramatic phenotype (Fig. 4, C and D). Considerably enlarged cells, up to four times the diameter of wild-type cells, were observed that showed intense 4′,6′-diamidino-2-phenylindole (DAPI) staining, indicative of elevated DNA content. In addition, a large number of "ghost" cells lacking DNA were seen (Fig. 4D). Flow cytometry of the cells containing overexpressed Vps4 (E206Q) revealed an aberrant profile with a significant proportion of the cells containing less than one or more than two genome equivalents. The cells with more than two chromosomes formed a broad continuum with non-integral genome contents, indicating that, in the absence of proper cell division, DNA replication is misregulated.

Here we have shown that *Sulfolobus* ESCRT system homologs play a role in the cell division process. The ESCRT system in human cells is involved in membrane abscission at the final stages of cytokinesis (*12*, *13*). However, there is no evidence of yeast ESCRT proteins being involved in cell division, leading to speculation that this role in human cells may be a recent evolutionary acquisition. Our findings suggest that the role of the ESCRT proteins in cell division may pre-date the divergence of the crenarchaeal and eukaryotic lineages and thus be reflective of the ancestral role of this complex. Just as

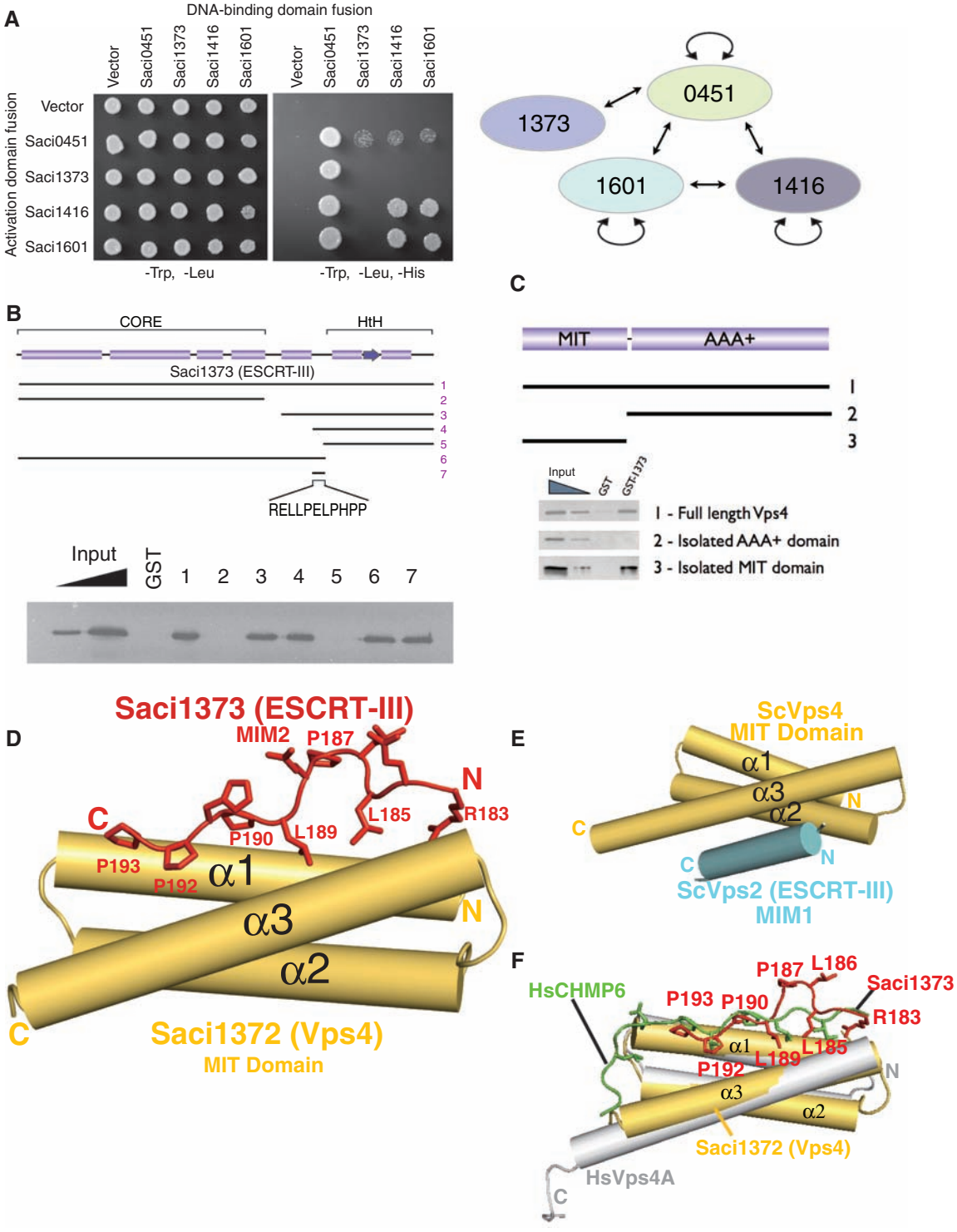

Fig. 3. (**A**) Interactions between ESCRT-III proteins detected by yeast two-hybrid analyses. Yeast cells containing the indicated plasmids were plated in media lacking leucine and tryptophan to select for plasmids and lacking histidine to score for interactions. (**B**) Identification of the minimal interaction site on Saci1373 (ESCRT-III) for binding Vps4. Glutathione *S*-transferase (GST) fusions of ESCRT-III fragments were used in pull-down assays with the full-length Vps4. The results of the pull-downs are shown in the lower panel. The input lanes contain 25 and 5% of input. (**C**) Identification of the interaction domain of Vps4 that binds Saci1373 (ESCRT-III). GST-Saci1373 (ESCRT-III) was used in pull-down assays with the full-length (1), C-terminal AAA+ domain (2), or isolated MIT domain (3) of Vps4. (**D**) A schematic representation of the interaction of Saci1373 (red) with the Saci1372 Vps4 MIT domain (yellow). (**E**) An illustration of the interaction of the yeast Vps4 MIT domain (yellow) with the C-terminal MIM1 motif (blue) of the yeast Vps2 ESCRT-III subunit. The MIM1 motif slots between MIT helices α2 and α3 (*14*). (**F**) The Saci1373 MIM2 (red)/Saci1372 MIT (yellow) interaction is closely related in structure with the CHMP6 MIM2 (green, extended)/VPS4A MIT (gray helices) interaction (*20*).

Downloaded from www.sciencemag.org on December 18, 2008

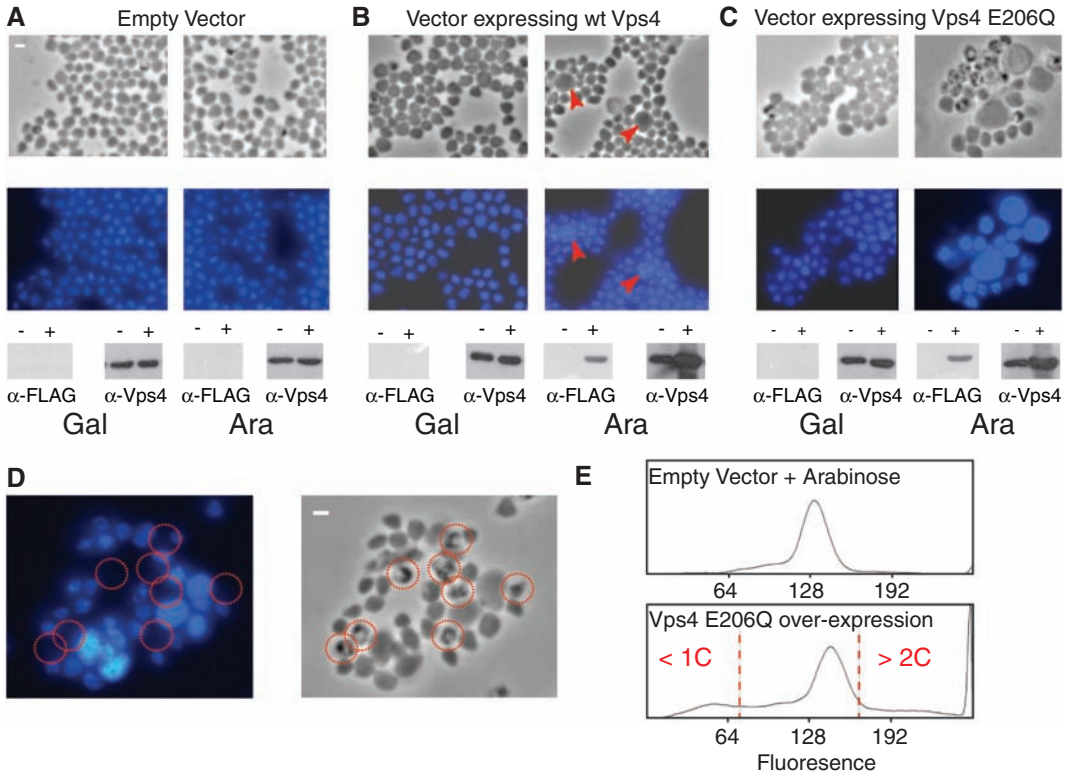

Fig. 4. (**A** to **C**) Phase contrast and fluorescent microscopy of DAPI-stained *S. solfataricus* cells containing either vector pRYS1 (A), pRYS1-wtVps4 (B), or pRYS1-Vps4 E206Q (C). In each panel, the left-hand images show cells grown in the repressing conditions (in the presence of galactose) and the right-hand images show cells in which expression of the plasmid-encoded gene is induced by the addition of arabinose. Red arrowheads in (B) indicate enlarged cells with elevated DNA content. The lower panels show the results of Western blotting with either antiserum to FLAG or antiserum to Vps4. The antiserum to the FLAG tag detects only the plasmid-encoded Vps4; the antiserum to Vps4 detects both plasmid and chromosomally encoded Vps4. The − and + symbols correspond to cells before and after the addition of either galactose (Gal) or arabinose (Ara). (**D**) An enlarged image of cells overexpressing Vps4 E206Q (phase contrast image on the left, fluorescent DAPI image on the right). Cells lacking discernable DAPI staining are circled in red. (**E**) Flow cytometric profile of cells grown in arabinose containing either empty vector or vector overexpressing Walker B (E206Q) Vps4. Cells with less than 1C or more than 2C genome content are indicated.

mammalian ESCRT-III subunits appear to have multiple roles in cell biology, the role of the archaeal ESCRT-III subunits may not be limited to cell division. Dominant-negative mammalian ESCRT-III subunits block HIV-1 budding and release (*10*, *22*). Indeed, a recent report revealed that the *S. solfataricus* ESCRT-III–like subunit Sso0881, the ortholog of Saci1416 (figs. S1 to 3), is associated with viral particles of the *Sulfolobus* turreted icosahedral virus (STIV) (*23*). Finally, the reduced complexity of the archaeal ESCRT apparatus provides a simplified model with which to investigate the core mechanisms of lattice formation and breakdown by this system.

References and Notes

1. M. B. Karner, E. F. DeLong, D. M. Karl, *Nature* **409**, 507 (2001).
2. C. M. Santelli *et al.*, *Nature* **453**, 653 (2008).
3. J. Pogliano, *Curr. Opin. Cell Biol.* **20**, 19 (2008).
4. N. A. Dye, L. Shapiro, *Trends Cell Biol.* **17**, 239 (2007).
5. W. Margolin, *Nat. Rev. Mol. Cell Biol.* **6**, 862 (2005).
6. R. Carballido-Lopez, J. Errington, *Trends Cell Biol.* **13**, 577 (2003).
7. J. Martin-Serrano, *Traffic* **8**, 1297 (2007).
8. R. L. Williams, S. Urbe, *Nat. Rev. Mol. Cell Biol.* **8**, 355 (2007).
9. R. C. Piper, D. J. Katzmann, *Annu. Rev. Cell Dev. Biol.* **23**, 519 (2007).
10. J. H. Hurley, S. D. Emr, *Annu. Rev. Biophys. Biomol. Struct.* **35**, 277 (2006).
11. C. Spitzer *et al.*, *Development* **133**, 4679 (2006).
12. J. G. Carlton, J. Martin-Serrano, *Science* **316**, 1908 (2007).
13. E. Morita *et al.*, *EMBO J.* **26**, 4215 (2007).
14. T. Obita *et al.*, *Nature* **449**, 735 (2007).
15. C. F. V. Hobel, S. V. Albers, A. J. M. Driessen, A. N. Lupas, *Biochem. Soc. Trans.* **36**, 94 (2008).
16. I. G. Duggin, S. McCallum, S. D. Bell, *Proc. Natl. Acad. Sci. U.S.A.* **105**, 16737 (2008).
17. See supplementary methods on *Science* Online.
18. Single-letter abbreviations for the amino acid residues are as follows: D, Asp; E, Glu; H, His; K, Lys; L, Leu; P, Pro; R, Arg; and X, any amino acid.
19. M. D. Stuchell-Brereton *et al.*, *Nature* **449**, 740 (2007).
20. C. Kieffer *et al.*, *Dev. Cell* **15**, 62 (2008).
21. J. M. Lubelska, M. Jonuscheit, C. Schleper, S. V. Albers, A. J. M. Driessen, *Extremophiles* **10**, 383 (2006).
22. K. Fujii, J. H. Hurley, E. O. Freed, *Nat. Rev. Microbiol.* **5**, 912 (2007).
23. W. S. A. Maaty *et al.*, *J. Virol.* **80**, 7625 (2006).

24. We thank O. Perisic and I. Duggin for advice and helpful discussions, C. Mueller-Dieckmann for help with European Synchrotron Radiation Facility beamline ID29, and S. McCallum for flow cytometry. The work was supported by the Wellcome Trust (grant 083639/Z/07/Z to R.L.W.), the Edward Penley Abraham Trust (S.D.B.). and the MRC (R.L.W. and S.D.B.). The coordinates for the structure reported in this work have been deposited in the Protein Data Bank (accession number 2w2u).

Supporting Online Material

www.sciencemag.org/cgi/content/full/1165322/DC1
Materials and Methods
Figs. S1 to S11
Tables S1 to S3
References
Movie S1

2 September 2008; accepted 3 November 2008
Published online 13 November 2008;
10.1126/science.1165322
Include this information when citing this paper.

De Novo Formation of a Subnuclear Body

Trish E. Kaiser,[1] Robert V. Intine,[1,2] Miroslav Dundr[1]*

The mammalian cell nucleus contains structurally stable functional compartments. We show here that one of them, the Cajal body (CB), can be formed de novo. Immobilization on chromatin of both CB structural components, such as coilin, and functional components of the CB, such as the SMN complex, spliceosomal small nuclear ribonucleoproteins (RNPs), small nucleolar RNPs, and small Cajal body–specific RNPs, is sufficient for the formation of a morphologically normal and apparently functional CB. Biogenesis of the CB does not follow a hierarchical assembly pathway and exhibits hallmarks of a self-organizing structure.

Compartmentalization of the nucleus contributes significantly to the regulation of nuclear functions (*1*–*5*). The structure of intranuclear compartments is maintained in the absence of defining membranes and despite a highly dynamic exchange of their components with the surrounding nucleoplasm (*6*, *7*). It has been suggested that nuclear bodies are formed by either an ordered assembly pathway or self-organization (*3*, *5*). To discriminate between these

Downloaded from www.sciencemag.org on December 18, 2008